A simple, sensitive and quantitative FACS-based test for SARS-CoV-2 serology in humans and animals

Agnès Maurel Ribes[1+], Pierre Bessière[2+], Jean Charles Guéry[3], Eloïse Joly Featherstone[4], Timothée Bruel[5], Remy Robinot[5], Olivier Schwartz[5], Florence Abravanel[3,6], Jacques Izopet[3,6] and Etienne Joly[7 *]

1 : Laboratoire d'Hématologie, Centre Hospitalier Universitaire de Toulouse, 31000, Toulouse, France
2 : Ecole nationale vétérinaire de Toulouse, Université de Toulouse, ENVT, INRAE, IHAP, UMR 1225, Toulouse, France
3 : Institut Toulousain des Maladies Infectieuses et Inflammatoires (Infinity), Université de Toulouse, INSERM, CNRS, UPS, 31300 Toulouse, France
4 : York University Hospital, York YO31 8HE, UK
5: Institut Pasteur, Virus and Immunity Unit, CNRS-UMR3569, Paris, France
6: Université de Toulouse, INSERM, CNRS, UPS, 31300 Toulouse, France
7: Institute of Pharmacology and Structural Biology (IPBS), University of Toulouse, CNRS, Toulouse, 31000, France

+: AMR and PB made equivalent contributions to this work.
*: correspondence to EJ: atnjoly@mac.com

Abstract

Serological tests are important for understanding the physiopathology and following the evolution of the Covid-19 pandemic. Assays based on flow cytometry (FACS) of tissue culture cells expressing the spike (S) protein of SARS-CoV-2 have repeatedly proven to perform slightly better than the plate-based assays ELISA and CLIA (chemiluminescent immuno-assay), and markedly better than lateral flow immuno-assays (LFIA).

Here, we describe an optimized and very simple FACS assay based on staining a mix of two Jurkat cell lines, expressing either high levels of the S protein (Jurkat-S) or the mCherry fluorescent protein (Jurkat-R, which serve as an internal negative control). We show that this Jurkat-S&R-flow test has a much broader dynamic range than a commercial ELISA test and performs at least as well in terms of sensitivity and specificity. Also, it is more sensitive and quantitative than the hemagglutination-based test HAT, which we described recently. The Jurkat-R&S-flow test requires only a few microliters of blood; thus, it can be used to quantify various Ig isotypes in capillary blood collected from a finger prick. It can be used also to evaluate serological responses in mice, cats and dogs. FACS tests offer a very attractive solution for laboratories with access to tissue culture and flow cytometry who want to monitor serological responses in humans or in animals, and how these relate to susceptibility to infection, or re-infection, by the virus, and to protection against Covid-19.

Introduction

Over the past year, our world has been thrown into disarray by a pandemic caused by a new coronavirus, SARS-CoV-2. With a mortality rate around 1%, this new virus is not as pathogenic as previous coronaviruses such as SARS-CoV (9.6%) and MERS (35%), but it transmits faster from human-to-human (Fani et al. 2020), probably because of a large proportion (ca. 50%) of asymptomatic carriers (Wu et al. 2021; Long et al. 2020). Consequently, in less than two years since its discovery in Wuhan, China, SARS-CoV-2 has spread all over the world and caused more than 200 millions confirmed cases and over 4 millions confirmed deaths (https://www.who.int/emergencies/diseases/novel-coronavirus-2019).

Biotechnology has proven a great asset in combating the pandemic, with the rapid development of diagnostic tests and, more recently, of vaccines. Diagnostic tests detect directly either the viral nucleic acid or viral proteins in nasopharyngeal swabs. Serological tests, by contrast, detect antibodies developed in response to infection by the virus or vaccination, or a combination of the two. Since the presence of antibodies in serum usually correlates with elimination of the virus and the patient's recovery, serological tests have not been very helpful in the clinic. They have, however, proven an essential tool to follow the spread of the pandemic by evaluating seroprevalence in populations, and they are now set to become essential to evaluate the immunity of individuals as well as populations (Koopmans and Haagmans 2020).

Whilst several thousands of studies have been published by now, based on serological tests performed in many millions of individuals, those myriad studies mostly document the seroprevalence in certain populations at a given time (Chen et al. 2021), but information regarding the actual protection afforded by immunity after infection by SARS-CoV-2, and how this correlates with the presence of antibodies against the SARS-2 virus is only just starting to come out (Lumley et al. 2021; Letizia et al. 2021; Abu-Raddad et al. 2021; Jeffery-Smith et al. 2021; R. A. Harvey et al. 2021; Garcia-Beltran et al. 2021).).

While these recent publications show that the presence of antibodies does correlate with protection against the Covid-19 disease, and in particular against the more serious forms of the disease, one of the more burning questions that remains to be answered is how long this protection will last? Another crucial question concerns whether there will be differences in the duration of this protection depending on which vaccine was used, and whether an individual had been infected by the SARS-CoV-2 virus before being vaccinated.

Obtaining answers to this type of questions should be greatly facilitated by access to simple, cheap and quantitative serological tests, which would work both in humans and in animal models. To date, however, although a multitude of commercial serological tests have been developed to detect the presence of antibodies in the serum of patients (Farnsworth and Anderson 2020), those are mostly ill-suited for use in research laboratories, not only because of their price, but also because they are not or only poorly quantitative.

The most commonly used methods for Covid-19 serodiagnostic are either ELISA (Enzyme-Linked ImmunoSorbent Assays) or CLIA (ChemiLuminescent ImmunoAssays). Whilst those methods show very good sensitivity and specificity, they also have several significant drawbacks:

i) The commercial versions are based on using volumes of serum or plasma which exceed the amounts which can be readily obtained by finger prick, and therefore require venipuncture, and hence trained personnel to collect the samples, and elaborate logistics to handle those samples.
ii) They are relatively expensive (ca. 500 € per plate of 90 tests for commercial ELISA or CLIA) and not easily modular (i.e. a whole plate will often have to be used even if only a few tests are to be performed). Whilst in-house ELISAs are a possible alternative, they are difficult to standardize and require high amounts of recombinant antigen (Amanat et al. 2020).
iii) Whilst ELISA tests are quantitative, they tend to saturate rapidly, and thus show a relatively limited dynamic range.
iv) Most commercial versions are designed to detect human antibodies, and thus cannot be used to follow serological responses in animal models.

Early in the pandemic, because they could be used in a point of care setting on capillary blood obtained by finger pricks, lateral-flow immune assays (LFIA) attracted considerable attention as an alternative to the ELISA or CLIA plate-based methods. Dozens of versions were developed by various commercial companies, and despite their relatively high price, such LFIAs were used in scores of studies to evaluate the prevalence of sero-conversion in various populations. Over time, however, the general performances of LFIAs have proven to be too low, both for sensitivity and reliability, to be of real use in clinical settings, and even for epidemiological studies (Adams et al. 2020; Mohit et al. 2021; Dortet et al. 2021; Moshe et al. 2021).

As an alternative to those various serological tests, we set out to develop a serological test based on hemagglutination, with the aim of obtaining a method that would be both sensitive, cheap, and could be used both in the laboratory, in field settings or as a point of care test, without the requirement for any elaborate equipment. The HAT (HemAgglutination Test) method is based on a single reagent, IH4-RBD, which binds to human red blood cells (RBC) via

114 the IH4 nanobody specific for human Glycophorin A and coats them with the RBD domain of the
115 SARS-CoV-2 virus (Townsend et al. 2021). HAT has a sensitivity of 90% and specificity of 99%,
116 and is now used by several laboratories worldwide for epidemiological and clinical studies
117 (Kamaladasa et al. 2021; Jayathilaka et al. 2021; Jeewandara et al. 2021). To be able to perform
118 HAT on whole blood with the sensitivity and simplicity which we set out the reach, and to
119 attempt to make it quantitative, various modifications and improvements had to be tested, and
120 in order to do this, we felt that we needed a simple quantitative test that would allow us to
121 evaluate the amount of antibodies present in the whole-blood samples we were using more
122 simply and cheaply than by using ELISA or CLIA.
123
124 In this regard, the S-flow test (Grzelak et al. 2020), which uses flow cytometry (FACS)
125 performed on human cells expressing the S protein, appeared as a very promising approach
126 since it is very simple to run and its performances compared favorably with three other
127 serological tests (two ELISA directed towards the S or N proteins, and a luciferase immuno-
128 precipitation system (LIPS) combining both N and S detection).
129 The S-flow method initially described used HEK cells (Grzelak et al. 2020), which are adherent
130 cells. We felt that it would be better to use cells growing in suspension, not only because it
131 makes it a lot easier to grow large numbers of cells, but also because those can be used directly,
132 without having to be detached from the plastic, which we feared could possibly alter the cells'
133 characteristics, and introduce a possible source of variability between assays.
134 In this regard, Horndler and colleagues have recently described an assay inspired by the S-
135 flow assay, but based on Jurkat cells expressing both the full-length native S-protein of SARS-
136 CoV-2 and a truncated form of the human EGFR protein, which is used as an internal control for
137 the expression level of the S protein (Horndler et al. 2021).
138 One of the caveats of using human cells to express the S protein, however, is that those cells
139 will also express other antigens, and MHC molecules in particular, which can be the targets of
140 allo-reactive antibodies present in certain individuals, and not others. The background level of
141 staining on Jurkat cells themselves will thus vary from sample to sample. To circumvent this
142 difficulty, Pinero et al. have used the Jurkat-S+EGFR cells mixed with untransfected Jurkat cells
143 as negative controls (Piñero et al. 2021).
144 Having followed the same reasoning as Horndler *et al.*, we had chosen to make use of Jurkat
145 cells expressing the native form of the spike protein of the SARS-CoV-2 virus, but we elected to
146 use Jurkat cells expressing the mCherry red fluorescent protein as negative controls. This is not
147 only cheaper because it does not require labelling the cells with an additional commercial
148 antibody, but also has the advantage of using two cell lines that are maintained in the same
149 selective tissue culture medium.
150 In all three papers (Horndler et al. 2021; Piñero et al. 2021; Grzelak et al. 2020), and several
151 others (Egia-Mendikute et al. 2021; Hambach et al. 2021; Lapuente et al. 2021; Goh et al. 2021),
152 the sensitivity of approaches based on flow cytometry was reported to be superior to those of
153 ELISA or CLIA, probably because such tests are based on detecting the spike protein expressed
154 in its native conformation.
155 Since the Jurkat-R&S-flow test calls for the use of both a flow cytometer and cells obtained
156 by tissue culture, it is clearly not destined to be used broadly in a diagnostic context, but its
157 simplicity, modularity, and performances both in terms of sensitivity and quantification
158 capacities should prove very useful for research labs working on characterizing antibody
159 responses directed against SARS-2, both in humans and animal models.

Results and Discussion

Jurkat-S&R-flow: basic principles

Jurkat cells expressing high levels of the SARS-CoV-2 spike protein, which we subsequently refer to as Jurkat-S, or J-S, were obtained by means of transduction with a lentiviral vector, followed by three rounds of cell sorting. A second population of Jurkat cells, in which all cells express the mCherry fluorescent protein, and which we subsequently refer to as Jurkat-R, or J-R, was also obtained by lentiviral transduction (see M&M: Materials and Methods section).

For the Jurkat-S&R-flow test, we simply prepare a mix of equivalent numbers of the two cells lines, J-S and J-R, and use either sera or plasma at a final dilution of 1/100 to label 2.10^5 cells of this mix (see M&M for details). After this primary step of labelling, the cells are washed before being incubated with a fluorescent secondary antibody, and a final wash is performed before analysis by flow cytometry.

The advantage of using such an approach is that it guarantees that the test cells (Jurkat-S) and the control cells (Jurkat-R) are labelled in exactly the same conditions. Comparing the levels of staining between test and control cells can then be carried out without any risk of a difference between the two being due to a difference in the course of the labelling procedure (e.g. less of the primary or secondary antibodies). Accessorily, another significant advantage of such an approach is that it reduces the number of FACS samples to be processed by a factor of two.

The mCherry signal allows simple separation by gating during analysis of the control cells from the test cells (Figure 1). In samples labelled just with the secondary antibody (neg. cont.) or with pre-pandemic plasma which does not contain antibodies against the spike protein (neg plasma), similar green signals are found on J-S et J-R populations. When there are antibodies against the spike protein present in the plasma or serum used to label the cells, this will result in a marked difference in the green signals detected on the J-S cells compared to the J-R cells. The difference in the fluorescence intensity between the two populations will provide a quantitative evaluation of the amounts of antibodies in the serum or plasma used to label the cells (first column). The numbers shown in red correspond to the relative specific staining (RSS = signal J-S – signal J-R / signal neg. cont.).

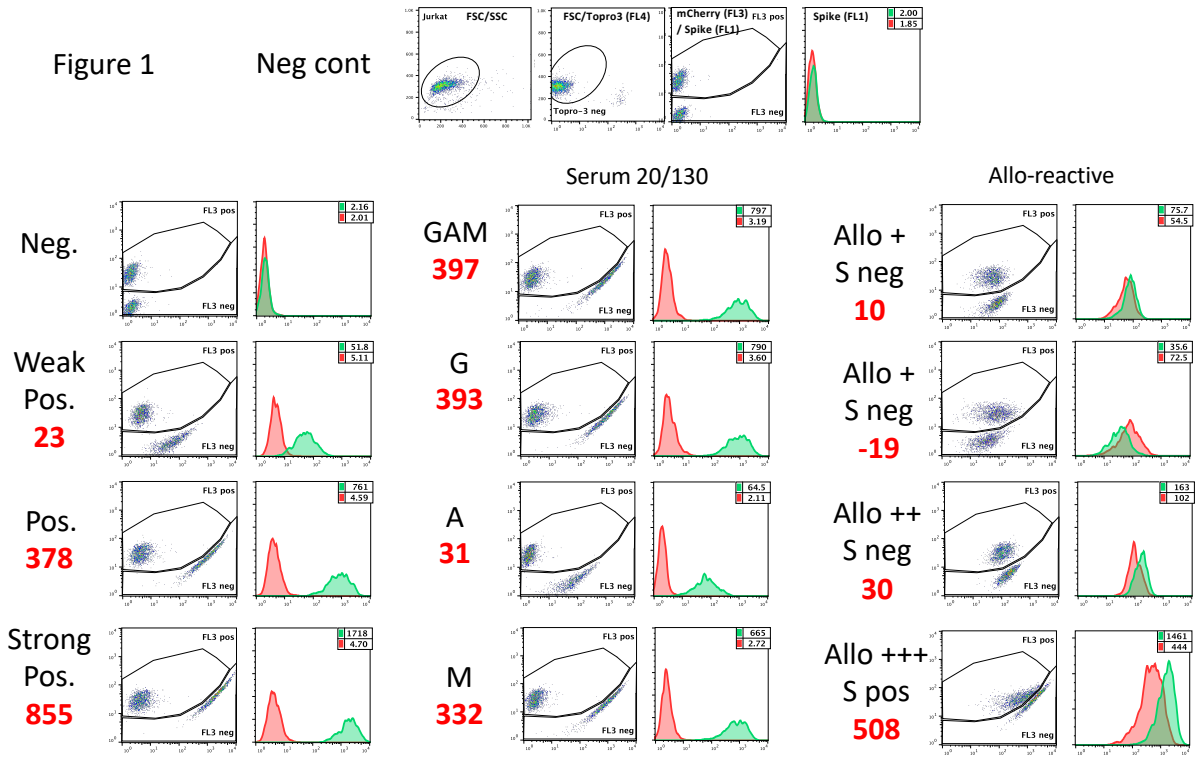

Figure 1: Basic principle and examples of the Jurkat-S&R-flow test

A 50/50 mix of Jurkat cells expressing either the S protein of the SARS-CoV-2 virus or the mCherry protein is first incubated with a 1/100 dilution of the plasma or serum sample to be tested, followed by incubation with a green fluorescent secondary antibody. The cells are then analyzed by flow cytometry.

The panels on the first line show the gating strategy, using as an example the sample of a negative control, stained only with an anti-human pan specific secondary antibody conjugated to alexa-488 : Live cells are first selected on a combination of two gates drawn on three parameters: size (FSC), granularity (SSC), and far red fluorescence (FL4) to eliminate the dead cells labelled by the Topro3 live stain. Jurkat-S are then distinguished from Jurkat-R cells using the red fluorescence of the latter, by means of a gate drawn on a FL1/FL3 dotplot. The gates had to be drawn that way to accommodate the fact that, for the brightest cells, the green fluorescent signal of alexa-488 can 'bleed' into the FL3 channel, and the Cellquest software does not allow for FL3/FL1 compensation. A histogram overlay is then drawn with the cells falling in each of these two gates (red: Jurkat-R, green: Jurkat-S). The numbers in the upper right corners of those histograms correspond to the GMFIs of the two histograms.

The red numbers shown to the left of the plots correspond to the relative specific staining (RSS; i.e. the difference of signal between J-S and J-R divided by the GMFI of the negative control, i.e. 2.00)

The first column shows examples of staining with 4 different plasmas which were either negative, or weakly, positively and strongly reactive with the spike protein.

The second column shows an example of the Jurkat-S&R-flow test capacity to perform a rough evaluation of the relative proportion of the various Ig isotypes in a sample, in this case the 20/130 reference serum obtained from the NIBSC.

The third column presents examples of some of the rare samples which showed various levels of allo-reactivity against the Jurkat cells themselves. Although the sample on the third line had an RSS of 30 (thus well above the threshold of 20 set for positivity), this sample was probably negative since it showed no reactivity in the other two serological tests. The sample on the fourth line shows that some sera can be both allo-reactive against the Jurkat cells, and strongly reactive against the spike protein.

223 If isotype-specific secondary reagents are used, an evaluation of the respective amounts of
224 various classes of antibodies can also be obtained (second column). It should, however, be
225 noted that, because different secondary reagents do not necessarily recognize the various Ig
226 isoforms with the same efficiency, this provides only a very rough analysis of the relative
227 amounts of Ig-G, -A and -M. Within a set of samples, however, this can provide very simple
228 means to compare samples with one another (Table S1).
229
230 As alluded to in the introduction, one of the possible caveats of using a human cell line to
231 express the S protein is that some blood samples will contain allo-reactive antibodies directed
232 against that cell line, possibly as a consequence of a pregnancy, or past history of receiving a
233 blood transfusion or organ transplant (Hickey et al. 2016; Karahan et al. 2020). The third column
234 of Figure 1 shows examples of such samples containing marked levels of alloreactive antibodies,
235 i.e. samples for which the J-R cells show significant levels of staining compared to the same cells
236 labelled with just the secondary antibody. Based on our results collected on more than 350
237 clinical samples, we evaluate that ca. 30 % of samples will contain allo-reactive Abs that will
238 result in levels of staining of Jurkat cells that are more than five-fold that of the signal obtained
239 for the negative control (and 3-6 % more than ten-fold). Of note, we did not notice an increased
240 frequency of allo-reactivity in samples from women compared to men, which suggests that allo-
241 reactivity after pregnancy is not a major cause in the origin of those allo-reactions.
242
243 A difficult question with all serological tests is that of where to set the threshold beyond
244 which the specific signals detected can confidently be considered as positive, which will be
245 directly linked to the balance between sensitivity and specificity of the assay. Based on the
246 analyses of various cohorts of positive and negative samples (some of which will be presented
247 further down in this manuscript), for the Jurkat-S&R-flow, we have settled for a threshold of RSS
248 =20, i.e. twenty-fold the value of the negative control stained just with secondary-antibodies.
249 The reason for using the geometric mean of fluorescence intensity (GMFI) of the negative
250 control as an internal reference is that, in flow cytometry, the numerical values of fluorescence
251 intensities will be totally dependent upon the cytometer settings, and the voltages applied to
252 the PMT in particular. But we find that this can be somewhat compensated by such an
253 approach. For example, in the conditions used in our experiments, the geometric mean of
254 fluorescence intensity (GMFI) of the negative control had a value of ca. 2 when analyzed on a
255 FACScalibur flow cytometer. With a threshold set at 20, samples were thus considered as
256 positive if the difference in the GMFI of the J-S and J-R populations was above 40 (numbers
257 shown in red in Figure 1 are J-S – J-R / 2). When the very same samples were analyzed on a
258 Fortessa flow cytometer (Figure S1), the value of the GMFI for the negative control was 24-fold
259 higher, but the RSS values obtained closely resembled those obtained with the same samples on
260 the FACScalibur (red numbers in Figure S1 and Figure 1: 20/23; 366/378; 916/855; 490/508).
261
262 For the samples showing high levels of allo-reactive staining, however, it is worth underlining
263 that this threshold of 20 had to be considered with some caution. Indeed, in those allo-reactive
264 samples, such as the examples shown in the right column of Figure 1, we found that the
265 difference between the green signals recorded for the J-S and J-R populations can fluctuate
266 between experiments, presumably because those signals correspond to the recognition by allo-
267 reactive antibodies of cell surface markers that are not always expressed at the same levels in
268 all Jurkat cells. Such alloreactive signals can be higher in J-R for certain serum or plasma

samples, or in J-S for other samples (first vs second and third line), without, in this latter case, necessarily corresponding to bona-fide reactivity against the spike protein of the SARS-CoV2 virus. The sample shown on the fourth line represents the most extreme case we have come across, from a Covid-19 patient with extremely high allo-reactivity, coupled to bona fide reactivity against the spike protein. All in all, it is simply worth underlining that, for the small percentage of samples showing significant alloreactivity against Jurkat cells, and staining of Jurkat-S slightly higher than that of Jurkat-R, their reactivity should be checked with a different serological test before considering them as truly positive.

Inspection of the dot plot for this very alloreactive sample provides the explanation for the slightly odd shapes of the FL1/FL3 gates we used to discriminate Jurkat-S from Jurkat-R cells. This was necessary because, on the FACScalibur, the fluorescent signal of mCherry is best captured by the FL3 channel, but the version of the Cellquest program used for acquisition on this cytometer does not allow for FL3/FL1 compensation. Consequently, samples with extremely high FL1 signals showed some 'bleeding' into the FL3 channel. We found that this could not be satisfactorily treated by post-acquisition compensation with the Flowjo analysis software either, and thus resorted to drawing such gates to separate J-S from J-R populations.

We had elected to use a green/red combination for test and control cells for two reasons: 1) secondary antibodies labeled with green fluorescent dyes such as fluorescein or Alexa 488 are the most commonly available, and also usually the cheapest. 2) All flow-cytometers, even the most basic ones, are equipped with a 488 nm laser which allows to perform green/red analyses. Another important consideration is that one of the goals of this study was to set up a test which could be used by as many research teams as possible, including those based in institutes from less affluent countries, which are less likely to have access to recent, state-of-the-art multi-laser flow cytometers.

When the same samples as shown on Figure 1 were analyzed using a Fortessa flow cytometer, the picture was quite different (Figure S1). This more recent flow cytometer is endowed with several lasers, including a 561 nm Yellow-Green laser, which is much better suited for the excitation of the mCherry fluorescent protein, thus yielding much higher signals which, since they are acquired on a different laser line from the green signals, require absolutely no compensation.

In many flow cytometry facilities, users are required to fix any samples that have been in contact with materials of human origin. Whilst this was not the case for us, we still tried analyzing the same samples after those were fixed with 1% formaldehyde and kept for 4 days at 4°C before re-analysis. As can be seen on the right part of Figure S1, formaldehyde-fixation resulted in a 7-fold drop in the intensity of the mCherry signals, which made it impossible to separate J-R from J-S population on the FACScalibur (first line). On the other hand, analysis on the Fortessa was still comfortably possible. Of note, whilst formaldehyde did not noticeably alter the fluorescence signals of the alexa-488 dye, it did result in a twofold increase of the green auto-fluorescence of the negative controls, hence resulting in a twofold reduction of the RSS compared to those obtained on unfixed cells.

315 ***Performance of the JurkatS&R-flow test on clinical samples***
316
317 Next, we compared the performance of the Jurkat-S&R-flow test with those of two other
318 serological tests: the Wantai commercial RBD ELISA test, and the hemagglutination-based test,
319 HAT (Townsend et al. 2021).
320
321 For this, we made use of two cohorts of clinical samples.
322 First, a preexisting cohort of 121 sera available in the virology laboratory of the Toulouse
323 hospital which had all previously been tested with the Wantai RBD ELISA test (Abravanel et al.
324 2020), comprising 40 negative serum samples collected before December 2020, and 81 sera
325 from PCR-positive subjects. For those samples, RBCs from O- donors were used to perform the
326 HAT tests (see M&M).
327 The second cohort consisted of 267 whole blood samples collected on EDTA, obtained from
328 the hematology department of the Toulouse hospital as left-over clinical material, for which we
329 has consequently very little clinical information. For those samples, the HAT test was performed
330 on whole blood, i.e. using the subjects' own RBCs for hemagglutination. The blood samples
331 were subsequently centrifugated, and the plasmas collected to perform the Jurkat-S&R-flow
332 and the RBD-ELISA tests.
333
334 The result of the analysis of these two cohorts with the three serological tests are presented
335 in Figure 2, with colors used to represent the HAT results.
336

Figure 2

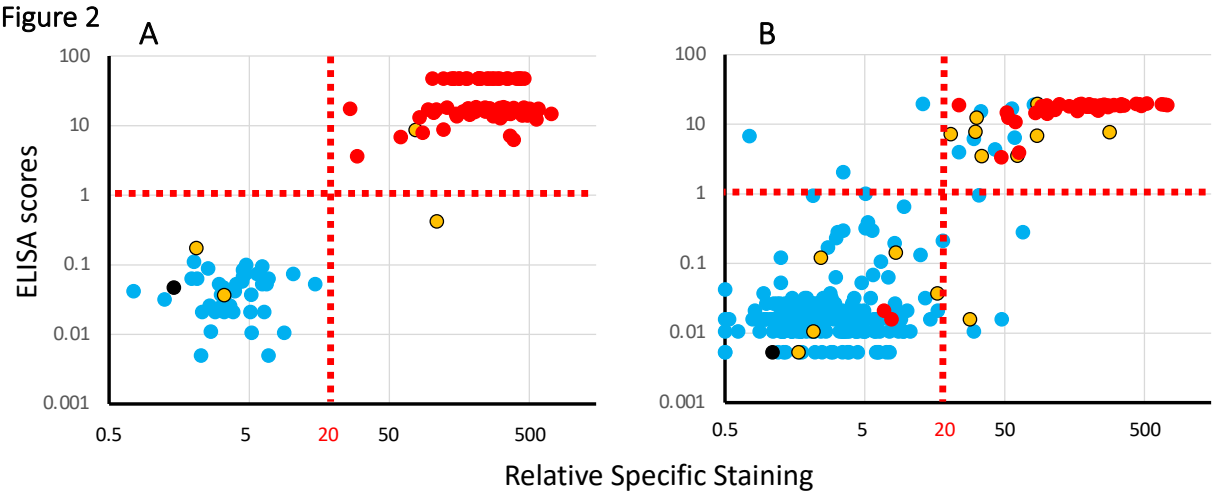

337
338
339 **Figure 2**: Comparison of the results of the 3 serological tests on two cohorts of clinical samples.
340 Panel A: results obtained with a cohort of 121 serum samples (81 PCR pos, 40 neg) collected by the
341 virology department of the Purpan Hospital (Toulouse, France).
342 Panel B: results obtained with a cohort of 267 whole blood samples coming from the hematology
343 department of the Rangueil Hospital (Toulouse, France).
344 Each plot presents ELISA scores (Y axis) against the results of the Jurkat-S&R-flow tests, expressed as RSS.
345 For improved clarity, both axes are presented on log scales (for this, the negative RSS values of 4 samples
346 of the cohort on the right had to be manually converted to a value of 0.5).
347 Colors are used to represent the HAT results: red: positive, blue: negative, yellow: partially positive
348 hemagglutination, black: false positive, i.e. samples for which hemagglutination also occurred with the
349 IH4 nanobody not coupled to the RBD domain.

The results of the first cohort (Figure 2A) show a clear-cut dichotomy in the distribution of the points, with two well separated clouds: one of blue points falling in the lower left quadrant, and one of red points in the upper right one. In other words, for this cohort of sera collected either from hospitalized Covid-19 patients or dating from before the pandemic for the negative controls, the three tests are in almost perfect agreement for the discrimination between positives and negatives, with just one yellow point in the lower right quadrant, i.e. positive for the Jurkat-S&R-flow test, showing only partial hemagglutination, but the signal for the RBD-ELISA test falling slightly below the threshold of 1 set by the manufacturer, suggesting that the anti-viral serological response of this subject was probably focused on regions of the spike protein outside of the RBD domain.

Of note, partial hemagglutination was also recorded for two other samples which were negative for the two other tests. Those two samples were from a group of 38 patients hospitalized for Covid-19, but for whom the blood had been collected less than 14 days after the PCR diagnostic. This observation is in line with our previous observation that the HAT test may be particularly performant for the detection of early serological responses, probably because of a higher hemagglutinating capacity of IgMs (Townsend et al. 2021). Incidentally, in this same group of 'early' PCR-positive Covid patients, there were also 4 other samples which were negative for all three tests (see tables of data provided as supplementary material).

The results of the second cohort, which comprised a few Covid patients, but also a large proportion of blood samples randomly picked among those from patients hospitalized for conditions unrelated to Covid-19, yielded a much less clear picture than the first one. As can be seen on Figure 2B, many of the dots for this cohort occupy a more intermediate position between the two clouds of clearly positive and clearly negative samples. In the upper right quadrant, one notices a relatively high proportion of blue and yellow spots, i.e. of HAT negative or partial samples in the set which were positive with both the RBD-ELISA and Jurkat-S&R-flow tests, albeit in the lower left part of the quadrant, i.e. rather weakly.

On the other hand, there are also a handful of samples in the lower left quadrant for which partial or full hemagglutination was detected, which may correspond to early serological responses. There are also a few blue dots in the upper left and lower right quadrant, thus corresponding to samples being positive only either with the RBD ELISA or the Jurkat-S&R-flow test. According to previous work, the sera which react weakly on the full length spike protein expressed at the surface of Jurkat cells are most likely due to cross-reactivities with the S2 domain of other coronaviruses (Ng et al. 2020; Khan et al. 2020).

One additional conclusion that can be drawn from the comparison of the results of the RBD-ELISA with those of the Jurkat-S&R-flow test is that, whilst the two methods show similar sensitivities, the ELISA signals tend to saturate very rapidly, and are thus much less dynamic that those obtained by flow cytometry.

393 ***Examples of possible uses of the Jurkat-S&R-flow test***
394
395 A further advantage of the Jurkat-S&R-flow test compared to the commercial RBD-ELISA we
396 used for this study is that it only requires 1 µL of plasma or serum, compared to 100 µL for the
397 ELISA, which makes it possible to perform on small volumes of capillary blood collected by finger
398 prick.
399

Figure 3

A

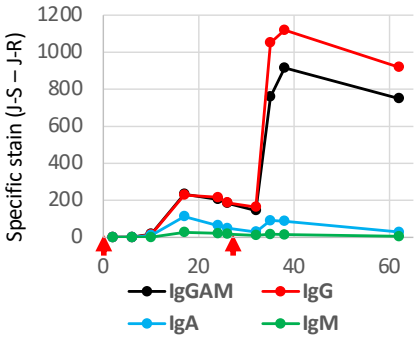

B

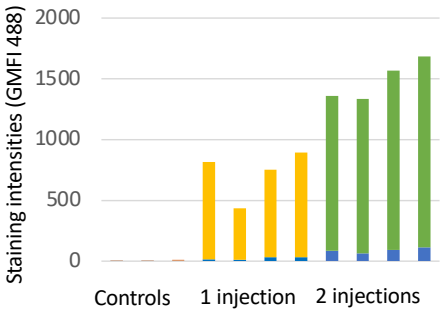

C

	Sample ID	GMFI J-S	GMFI J-R	Specific stain	Neutralisation titers
Sera from exposed Cats	neg cont	2.06	1.87	0.19	
	PNRA	12.5	15.4	2.9	-
	VK8X	9.04	15.7	6.66	-
	MPP5	10.6	18	7.4	-
	NATW	51.7	64.5	12.8	-
	XEPP	36.2	55	18.8	-
	20-059	14.3	57.4	43.1	-
	79UQ	25.8	71.7	45.9	**1:400**
	NP3W	15.2	73.6	58.4	**1:200**
	66JQ	30.6	642	611.4	**>1:1280***
	AMGT	47.6	679	631.4	**1:100**
	GTVJ	24.3	730	705.7	**1:400**
Sera from exposed Dogs	neg cont	1.93	1.85	0.08	
	GMLX	25.9	14	11.9	-
	KDEJ	34.6	19.8	14.8	-
	ZVJX	38.8	23.7	15.1	-
	4USK	50.1	32.5	17.6	**1:100**
	DP5K	44.6	20.7	23.9	-
	0006	54.1	29.7	24.4	-
	XXHT	55.6	13.4	42.2	**1:200**
	RUML	64.4	10.3	54.1	**1:200**
	BTFP	87.9	9.72	78.18	**1:100**
	KJY8	136	9.82	126.18	**1:200**
	CSSL	246	6.24	239.76	**1:200**

400
401 **Figure 3**: Various examples of the possible uses of the Jurkat-S&R-flow test
402
403 **Panel A**: Monitoring serological responses in humans
404 The Jurkat-S&R-flow test was used to follow the serological response of an individual during the
405 course of his vaccination (red arrows: first injection on day 0 and boost on day 27), with isotyping using
406 specific secondary reagents performed as described in the M&M section. Y axis: Specific staining (GMFI
407 J-S – GMFI J-R)
408
409 **Panel B**: The Jurkat-S&R-flow test can be used to follow Ig responses in mice.
410 Sera from three groups of mice having been immunized either once, twice or not by intra-peritoneal
411 injection of inactivated SARS-CoV-2 virus were analyzed with the Jurkat-S&R-flow test, using an anti-
412 mouse Ig secondary antibody. Y axis: GMFI on Jurkat-R (blue columns), on Jurkat-S (top of green
413 columns), The specific signals correspond to the yellow or green portions (GMFI J-S – GMFI J-R).
414
415 **Panel C**: In cats and dogs, the results of the Jurkat-S&R-flow test correlate with those of sero-
416 neutralization titers.
417 Panels of sera from cats and dogs whose owners had recovered from symptomatic Covid-19 were
418 used to perform both sero-neutralization assays and the Jurkat-S&R-flow test, using the corresponding
419 secondary antibodies. Specific stain = GMFI J-S – GMFI J-R. *: the higher SN titers shown for the cat
420 serum 66JQ was obtained on a different day from all the others.

421 As a proof of concept that this was doable and useful, we used capillary blood which one of
422 the authors collected by pricking his finger at various intervals to document the time course of
423 his serological response after vaccination, and the results are shown in panel A of Figure 3. One
424 somewhat surprising finding was with the low levels of IgM recorded, which may in part be
425 explained by the fact that, as a rule, anti-IgM secondary antibodies tend not to work as well as
426 those against the other isotypes. One should note, however, that, with the same anti-IgM
427 secondary reagent, signals of the same order of magnitude were found for IgG and IgM with the
428 20/130 reference serum (Figure 1), as well as in several other samples (Table S1). The
429 observation that the signals obtained with an anti-IgG reagent are similar, and even often a bit
430 higher to those obtained with the pan-reactive anti-IgGAM is something which we tend to find
431 in most samples (Table S1), and which had already been underlined by Grzelak et al. in the
432 context of the S-flow test (Grzelak et al. 2020).
433
434 The capacity of the SARS-CoV-2 virus to infect primates, hamsters or ferrets has provided
435 very useful animal models to understand the physiopathology of Covid-19, whilst its capacity to
436 infect domestic pets such as cats and dogs does raise concerns about the transmissions of the
437 virus back to humans, as well as about the problem of animal reservoirs from which it will be
438 very difficult to eradicate the virus. Whilst scores of commercial and lab-made methods have
439 been described to follow human serological responses to the virus, there is a remarkable
440 paucity of tests available today applicable to animals. Since all it would take to adapt the Jurkat-
441 S&R-flow test to animals would be to use different species-specific secondary antibodies, we
442 explored whether this would work for mice, cats, and dogs.
443
444 First, we used sera of mice which had been immunized once or twice with inactivated SARS-
445 CoV-2 virus injected intra-peritoneally. As can be seen on panel B of Figure 3, whilst the sera of
446 control mice did not react significantly with Jurkat cells, those of immunized mice showed
447 strong specific reactions against the spike protein, which were even higher in those having
448 received two injections. Of note, the reactions against the Jurkat-R cells also went up in
449 correlation with the injections, albeit to a much lesser degree than against the S protein. This is
450 presumably due to the fact that the preparations of inactivated virus used for the
451 immunizations probably contained some bovine proteins from the serum used in the tissue
452 culture medium that would have the capacity to bind to the surface of the Jurkat cells, such as,
453 for example, beta-2-microglobulin binding to MHC class I molecules. The Jurkat-S&R-flow
454 method therefore seems to work very satisfactorily in mice, and since it requires only a few µL
455 of blood, it is well suited to follow serological responses over time.
456
457 We then turned our attention to cats and dogs, which have both been shown to be
458 susceptible to infections by the SARS-CoV-2 virus (Sit et al. 2020; Dróżdż et al. 2021; Bessière et
459 al. 2021; Chen 2020), but for which one of the only reliable means to test for the presence of a
460 serological response is to perform sero-neutralization experiments, which are both
461 cumbersome and require access to BSL-3 facilities. For our exploratory experiments, we simply
462 used sets of sera collected from 11 cats and 11 dogs whose owners had had symptomatic Covid-
463 19 infections, and on those we performed both sero-neutralization experiments, and the Jurkat-
464 S&R-flow test, using the appropriate secondary antibodies. As can be seen on panel C of Figure
465 3, we found a very good correlation between the levels of specific staining of Jurkat-S cells and
466 the neutralization titers of the same sera. Whilst those are very preliminary observations which

467 will need to be strengthened by many more samples, and in particular with samples collected
468 before the Covid-19 pandemic as negative controls, those results show that the Jurkat-S&R-flow
469 test can clearly be used to evaluate the levels of antibodies against the S protein of the SARS-
470 CoV-2 virus in cats and dogs, and could presumably also be adapted to other animals, be they
471 pets, farm animals or laboratory models used to study the viral infection.
472

473 ## Concluding remarks and perspectives

474

475 Given its versatility, flexibility and affordability, we believe that the Jurkat-S&R-flow assay
476 could prove useful for many research scientists wanting to measure serological responses
477 directed towards the spike protein of the SARS-CoV-2 virus, either in humans, or in animals, but
478 who would not have either the financial means to purchase commercial plate-based assays such
479 as ELISA or CLIA, or access to the sizeable amounts of recombinant proteins required to set
480 those up in-house. The Jurkat-S&R-flow test could be performed by any laboratory with access
481 to tissue culture and to a flow cytometer, at a cost of roughly 10 cents per sample (see M&M for
482 calculation). It is thus much cheaper than commercial ELISAs, which cost around 500 € per plate
483 of 90 samples. And the Jurkat-S&R-flow test is also completely modular, i.e. each test only
484 comprises the number of samples required, contrary to plate-based assays for which it is rather
485 difficult not to use up a whole plate every time.
486

487 Several reports have already highlighted that using flow-cytometry for the detection of
488 antibodies binding to the S protein expressed at the surface of cells tends to perform better
489 than plate-based assays which use immobilized recombinant proteins (Egia-Mendikute et al.
490 2021; Hambach et al. 2021; Lapuente et al. 2021; Goh et al. 2021; Horndler et al. 2021; Piñero et
491 al. 2021; Grzelak et al. 2020; Ng et al. 2020). This is most likely related to the fact that many
492 antibodies will be binding to conformational epitopes, which will only be found on the naturally
493 expressed and properly folded spike protein. In this regard, the capacity of the S protein to
494 undergo structural fluctuations, particularly at the level of the RBD domain which can be in
495 either an open/up or closed/down conformation, has been shown to influence the binding-
496 capacity of various antibodies (W. T. Harvey et al. 2021; Barnes et al. 2020; Robbiani et al. 2020;
497 Piccoli et al. 2020; Zhou et al. 2020; Huang et al. 2021; Dejnirattisai et al. 2021). This is
498 supported by the results shown in Figure S2, i.e. that, for most samples, we found that
499 incubation at room temperature resulted in a sizeable increase in the amounts of antibodies
500 binding to the spike-expressing cells, suggesting that, at the surface of live cells, the capacity of
501 the spike protein to fluctuate between various conformations will expose different epitopes,
502 and allow the binding of more antibodies.
503

504 One striking aspect of the results shown on Figure 2 is in the difference of performance of
505 the tests between the two cohorts of samples tested. On the one hand, nearly perfect scores
506 were obtained for all three tests on a cohort of sera comprised either of control samples
507 collected before 2019, or of positive sera from PCR-positive Covid-19 patients. On the other
508 hand, the situation was much less clear-cut for the cohort comprising blood samples picked
509 more or less randomly and blindly among those available as left-overs from the hematology
510 department and was, therefore, more akin to a 'real' population. For this second cohort, an
511 additional confounding factor may have been that, since all the samples were from hospitalized

512 patients, some sera may have been poly-reactive due to inflammatory pathologies unrelated to
513 Covid-19.
514
515 All in all, this difference between the two cohorts is reminiscent of the common observation
516 that the performances of clinical tests are often much lower on real populations than those
517 obtained by the manufacturers on very carefully controlled and standardized populations. Our
518 results indeed bring support to the view that the performance of any given serological test will
519 be entirely dependent on the set of samples used to measure it: whilst it is relatively easy to
520 reach an almost perfect score on a cohort comprised only of highly positive and completely
521 negative samples such as the one used for Figure 2A, the situation becomes much less clear
522 when using a set of samples more closely resembling the general population, in which the
523 positive or negative nature of many samples will remain uncertain, and from which it would
524 thus seem futile to try to make precise calculations of sensitivity and specificity. This being said,
525 performing several tests in parallel on such cohorts is very useful to compare the performance
526 of those tests with one another.
527
528 Several recent reports have underlined the correlation between the serological levels of
529 neutralizing antibodies, which are mostly directed against the RBD, and the degree of protection
530 against becoming infected, or re-infected, by the SARS-Cov-2 virus (Feng et al. 2021; Khoury et
531 al. 2021; Garcia-Beltran et al. 2021). Low levels of antibodies are often found in convalescent
532 subjects following asymptomatic infections, and Kalamadasa and colleagues have shown that,
533 whilst HAT sensitivity in such individuals can be as low as 50 %, HAT results are strongly
534 correlated with the seroneutralisation activity in those samples (Kamaladasa et al. 2021). Over
535 the coming months and years, antibodies levels will progressively decrease in both vaccinated
536 and convalescent people, and one of the crucial questions will be that of when to start planning
537 to administer vaccine boosts. Levels of neutralizing antibodies will certainly evolve very
538 differently in different individuals, and an additional difficult aspect will be to define rules for
539 the administration of vaccine boosts, and whether those should be defined as a general rule
540 (e.g. so many months after the initial vaccination), or individually, based on the monitoring the
541 levels of neutralizing antibodies. For such an individually-based approach, HAT would seem to
542 be a particularly appropriate solution since it is a very simple and cheap test based on the
543 binding of antibodies to the RBD domain (Townsend et al. 2021), which are those with
544 neutralizing activity. Furthermore, because the only reagent in HAT simply comprises small
545 amounts of soluble IH4-RBD protein , the hemagglutination test can be very easily adapted to
546 detect antibodies binding to variant forms of the virus (Jayathilaka et al. 2021).
547 Whilst HAT is not as sensitive as an anti-RBD ELISA or the Jurkat-S&R-flow test, this relatively
548 low sensitivity may not really be a problem for using HAT to help decide when to revaccinate
549 people since low levels of antibodies are unlikely to be fully protective. By performing titrations,
550 the HAT assay can also provide a quantitative assessment of the levels of circulating antibodies,
551 which have been shown to correlate strongly with sero-neutralisation titers (Lamikanra et al.
552 2021). In the current version of HAT, however, such a quantification can only be performed in a
553 laboratory environment because it requires separation of the plasma or serum from the red
554 blood cells. Making use of the Jurkat-S&R-flow test as a reference, we are currently in the
555 process of completing work on a modified version of HAT that will be compatible with being
556 performed pretty much anywhere, with no specialized equipment, and will provide a
557 quantitative evaluation of the levels of antibodies in a single step (Joly et al. man in prep.).

558 **Detailed Contributions**

559

560 **Authors**

Name	First name	ORCID	contributions
Maurel Ribes	Agnes	0000-0002-7560-9502	Collected and anonymized blood samples; scored HAT tests, corrected the manuscript
Bessière	Pierre	0000-0001-5657-0027	Provided cat and dog sera; performed SN; helped perform FACS assays, corrected the manuscript
Guéry	Jean Charles	0000-0003-4499-3270	Provided immunized mouse sera; corrected the manuscript
Joly Featherstone	Eloise	0000-0001-9077-359X	Scored HAT tests
Bruel	Timothée	0000-0002-3952-4261	Provided Jurkat-R and -S cells; corrected the manuscript
Robinot	Rémy	0000-0002-3651-0171	Transduced, selected and grew Jurkat cells
Schwartz	Olivier	0000-0002-0729-1475	Provided Jurkat-R and -S cells
Abravanel	Florence	0000-0002-1753-1065	Provided cohort of sera and ELISA kits
Izopet	Jacques	0000-0002-8462-3234	Provided cohort of sera and ELISA kits; made suggestions for the manuscript
Joly	Etienne	0000-0002-7264-2681	Designed and funded the study; Performed the experiments; Wrote the paper.

561

562 **Other contributors**

Townsend	Alain	Designed the IH4-RBD reagent and funded its production
Tiong	Tan	Produced the IH4-RBD reagent
Rijal	Pramilla	Produced the IH4-RBD reagent
Buchrieser	Julian	Generated lentiviral vectors
Porrot	Françoise	Grew Jurkat cells
Featherstone	Carol	Copy edited parts of the manuscript

563

564 ## Acknowledgements

565

566 The authors are extremely grateful to Alain Townsend, Tiong Tan, Pramila Rajal, Julian
567 Buchrieser and Françoise Porrot, who contributed the various materials detailed in the above
568 table, and to Carol Featherstone for copy editing the manuscript. They also gratefully
569 acknowledge the contributions of Marianne Navarra, for her help in setting up the agreement
570 with the hospital; Miriam Pinilla, Karin Santoni and Etienne Meunier for the gift of Topro-3 and
571 for performing the Mycoplasma tests; Emmanuelle Naser and Penelope Viana from the IPBS
572 flow cytometry facility for their assistance, and the very helpful staff of the Toulouse EFS.

573

574 Funding: The first part of this project was funded by a private donation. The second part was
575 funded by the ANR grant HAT-field to EJ.

576 **Materials and Methods**
577
578 **Reagents**
579
580 Polyclonal anti-human and anti-mouse Igs secondary antibodies, all conjugated to Alexa-488,
581 were from Jackson laboratories, and purchased from Ozyme (France) . Refs: anti-human Ig-
582 GAM: 109-545-064, -G: 109-545-003, -A: 109-54-011, -M: 109-545-129; anti-mouse Ig-G: 115-
583 545-003
584
585 Anti-cat IgG (F4262) and anti-dog IgG (F7884) secondary antibodies, both conjugated to FITC,
586 were obtained from Sigma.
587
588 Anti RBD monoclonal antibodies: FI3A (site 1) and FD-11A (site 3) (Huang et al. 2021); C121
589 (site 2) (Robbiani et al. 2020); CR3022 (site 4) (ter Meulen et al. 2006); EY6A (site 4) (Zhou et al.
590 2020). All those were obtained using antibody-expression plasmids, as previously described
591 (Townsend et al. 2021).
592
593 The 20/130 WHO reference serum was obtained from the NIBSC (Potters Bar, UK)
594
595 BSA Fraction V was obtained from Sigma (ref A8022).
596
597 PBS and tissue culture media were obtained from Gibco.
598
599 **Generation of Jurkat-S and Jurkat-R cell lines**
600 Both cell lines were obtained by means of lentiviral transduction.
601 pLV-EF1a-SARS-CoV-2-S-IRES-Puro was created by cloning a codon-optimized version of the
602 SARS-CoV-2 S gene (GenBank: QHD43416.1) into the pLV-EF1a-IRES-Puro backbone (Addgene
603 plasmid # 85132 ; http://n2t.net/addgene:85132 ; RRID:Addgene_85132) using BamHI and
604 EcoRI sites.
605 The lentiviral vector for the expression of mCherry was obtained by replacing the GFP
606 sequence of GFP by that of mCherry in the pCDH-EF1α-MCS*-T2A-GFP plasmid
607 (https://systembio.com/shop/pcdh-ef1α-mcs-t2a-gfp-cdna-single-promoter-cloning-and-
608 expression-lentivector/)
609 Lentiviral infectious supernatants were obtained after transient transfection of HEK cells with
610 pLV- or pCDH-derived vectors, together with the packaging R8-2, and VSV-G plasmids.
611 Supernatant was harvested 24h and 48h post transfection, passed through a 45 µm filter and
612 stored in aliquots at -80°C. For the transduction of Jurkat cells, those were distributed in a 6 well
613 plate at 1.5. 10^6 cell per well, in a volume of 500 µL of tissue cuture medium (RPMI, 10 % FCS,
614 1% PS, 2% Hepes), and 20 µL of the infectious supernatants were added, as well as 5 µL of
615 Lentiblast premium (OZBiosciences). The plate was then spun at 1000g for 60 min at 32°C,
616 before adding 2.5 ml of tissue culture medium and returning the plate to the 37°C incubator.
617 Selection with puromycin was then performed at a concentration of 10µg/mL.
618 After a few days, the population of Jurkat cells thus obtained was stained for flow cytometry
619 analysis using a highly reactive serum from a covid-19 patient, and it was found that most cells
620 expressed the S protein, but at low to intermediate levels. To obtain a population that would
621 express higher levels, we submitted this population to three successive rounds of sterile cell

622 sorting using a FACSAria Fusion cell sorter (Beckton Dickinson), selecting each time the 5 % of
623 cells with the brightest staining. Cells were placed back in culture and reamplified after each
624 round of selection. At the time of the second round of sorting, the cell sorter was also used for
625 single cell cloning, but all of the dozen clones obtained by this means showed lower expression
626 that the sorted population. The expression of the S protein in the population of Jurkat cells
627 obtained after these three rounds of sorting was found to remain expressed in all cells, and at
628 similar levels, for more than 50 successive passages, over many weeks of continuous cell
629 culture.
630
631 The Jurkat-R cells were obtained by successive transduction with the pCDH-GFP lentiviral
632 vector described above, then with the empty pLV lentiviral vector, followed by selection with
633 Puromycin at 10µg/mL. FACS analysis revealed that the mCherry fluorescent protein was
634 expressed in 100 % of the cells of the population thus obtained, which therefore did not need to
635 undergo any cell sorting.
636
637 After the initial selection process, both the Jurkat-S and Jurkat-R cell line were maintained in
638 RPMI, 10 % FCS, 2 mM Glutamine, 1% PS and Puromycin at 2.5 µg/mL. The Jurkat-S and Jurkat-R
639 cell lines were both checked for the absence of mycoplasma contamination using the HEK blue
640 hTLR2 kit (Invivogen, Toulouse, France)
641
642 **FACS staining**
643 Before experiments, cells in the cultures of both Jurkat-S and Jurkat-R cell lines were
644 counted, and sufficient numbers harvested to have a bit more than 10^5 cells of each per sample
645 to be tested. Cells from both cell lines were then spun, and resuspended in their own tissue
646 culture medium at a concentration of 2.2 10^6 cells/ mL before pooling equal volumes of the two.
647 Plasmas or sera to be tested were diluted 1/10, either in PBS or in PFN (PBS / 2% FCS / 200
648 mg/L sodium azide). 10 µL of these 1/10 dilutions were then placed in U-bottom 96 well plates,
649 before adding 90 ul per well of the Jurkat-S&R mix.
650 The plates were then incubated for 30 minutes at room temperature before placing them on
651 ice for a further 30 minutes. As can be seen on the supplementary Figure 2, we have found that
652 this initial incubation at room temperature results in a marked increase of the staining signals
653 for most antibodies.
654 All subsequent steps were carried out in the cold, with plates and washing buffers kept on
655 ice. After the primary staining, samples were then washed in PFN, with resuspending the cells
656 by tapping the plate after each centrifugation, and before adding the next wash. After 3 washes,
657 one drop (i.e. ca. 30 ul) of secondary fluorescent antibody diluted 1/200 in PFN was added to
658 each well, and the cells resuspended by gentle shaking of the plates.
659 After an incubation of 60 min on ice, samples were washed two more times with cold PFN
660 before transferring the samples to acquisition tubes in a final volume of 300 ul PFN containing
661 30 nM TO-PRO™-3 Iodide (Thermo Fischer Scientific, ref T3605).
662 This protocol was used for staining with just one pan-specific secondary antibody, i.e. for
663 most of the samples of this study. For specific isotyping, i.e. for staining separately with either
664 anti-IgG, -IgA or -IgM, as well as the pan-specific anti-Ig-GAM secondary antibody, we used
665 double the quantities of cells and of serum or plasma for the primary step, and split the samples
666 into 4 wells after the second wash, before proceeding to the subsequent steps as for the
667 standard protocol.

668 The vast majority of the experiments for this study were analyzed on a FACScalibur flow
669 cytometer controlled by the Cellquest pro software (Version 5.2, Beckton Dickinson), using the
670 FL1 channel for Alexa-488 or FITC, the FL3 channel for m-Cherry, and the FL4 channel (with the
671 633 nm laser) for live gating with the TO-PRO™-3 live stain.
672 For the samples shown on supplementary Figure 1, double quantities were used (as for
673 isotyping) so that the same samples could also be acquired on a Fortessa flow cytometer,
674 controlled by the Diva software (Beckton Dickinson). After the samples had been run on both
675 machines, an equivalent volume of PBS with 2% formaldehyde what added to what was left in
676 the tubes, and those were stored at 4°C for 4 days before they were once again analyzed on
677 both machines.
678 Post-acquisition analysis of all the samples was performed using the Flowjo software (version
679 10.7.1)
680
681 **Cost of the Jurkat-S&R-flow test**
682 The cost per sample of the Jurkat-S&R-flow test lies in large part with the price of the
683 secondary antibodies used. Typically, one vial of secondary antibody costs about 150 € for 1ml,
684 and using 30-50 ul at a 1/200 dilution will provide for at least 5000 samples. The cost of a
685 polyclonal antibody is thus of the order or 3-5 cts per sample.
686 Each sample requires 2.10^5 jurkat cells, which is roughly the amount obtained with 0.5 ml of
687 standard tissue culture medium, which costs around 50 €/L, i.e. 2.5 cts/sample. All in all, if one
688 adds the cost of TC, buffers for the washes and disposable plastics, we estimate that the cost
689 per sample will be of the order of 10 cts.
690 The cost of access to a flow cytometer will be extremely variable between laboratories and
691 institutes. If the cost of access is 20 € per hour, and one runs 200 samples per hour, this will add
692 another 10 cts to the cost per sample.
693
694 **HAT tests**
695 HAT tests were performed using the IH4-RBD reagent diluted at 1 ug/ml in PBN rather than in
696 straight PBS as originally described (Townsend et al. 2021), which results in a slight
697 improvement of the HAT performances, and much improved stability of the IH4-RBD stocks (
698 Joly et al., man in prep.). PBN simply consists of PBS complemented with 1% BSA and 200 mg/L
699 sodium azide. The main role of BSA is to prevent the IH4-RBD reagent from adsorbing onto the
700 plastic of tubes and assay plates, and the azide prevents bacterial and fungal contaminations of
701 the stocks. HAT tests were all performed in V-bottom 96 wells plates (Sarstedt, ref 82 1583).
702 For performing HAT on sera, two tubes of suspension of RBC from an O- donor were
703 prepared at approximately 6µL of packed RBC per ml of PBN. The first tube was used to fill the
704 negative control wells with 90 µL per well. The IH4-RBD reagent was added at 1.1 ug/ml to the
705 second tube of RBC suspension and this was dispensed at 90 µL per test well. Sera to be tested
706 were diluted 1/10 in PBS, and 10 µL of the dilutions were added to a control and a test well.
707 For performing HAT on whole blood samples, which were all leftover clinical samples
708 collected in EDTA tubes (purple tops), 10 µL were diluted with 60 µL of PBS + 5 mM EDTA, and
709 10 µL of this 1/7 dilution were added to each of two wells containing either 90 µL of PBN for the
710 negative controls, or 90 µL of PBN containing 1.1 µg/mL of IH4-RBD reagent for the test wells.
711

712 For both sera and whole blood samples, after 60 minutes incubation at room temperature,
713 the V bottom plates were placed on a homemade light box tilted at an angle of approximately
714 10° from the vertical, and pictures taken with a mobile phone after approximately 20 seconds.
715 In an attempt to increase the sensitivity of the method by detecting partial
716 hemagglutinations, the plates were then returned to a horizontal position for a further two
717 hours, and the procedure of tilting the plate and taking pictures was repeated.
718 After transferring the pictures to computer files, the hemagglutination tests were scored by
719 three independent assessors, of which two were blinded.
720 The scoring system was as follows: A score of 1 was given only to those samples which
721 showed complete hemagglutination after one hour. A score of 0.5 was given to samples which
722 showed either partial hemagglutination after one hour, or partial or complete hemagglutination
723 after the second incubation of 2 hours.
724 This revealed that, whilst there was 100% agreement between the three assessors for the
725 scoring of complete hemagglutination, the scoring of partial hemagglutination proved to be
726 much more subjective and variable, and only those samples which had been scored as partials
727 by all three assessors were finally considered as bona fide partial hemagglutinations.
728
729 **ELISA**
730 The ELISA tests were performed using the WANTAI SARS-CoV-2 Ab ELISA (ref WS-1096),
731 according to the manufacturer's instructions. This commercial kit allows detection of all human
732 antibody isotypes recognizing a recombinant RBD domain of the SARS-Cov-2 virus.
733 The ELISA tests for the cohort of 121 sera were performed in the virology department of the
734 Toulouse hospital, as described previously (Abravanel et al. 2020).
735 The series of ELISA tests for the cohort of 267 plasmas were performed at the IPBS, with the
736 washes being performed by hand rather than by an automated machine, and the 450/625 ODs
737 read by a µQuant plate reader. All the positive samples of this cohort, as well as a set of
738 randomly selected negatives, were submitted to a repeat of the assay, which showed excellent
739 reproducibility.
740
741 **Human samples**
742 Purpan cohort: The collection of 2019 (negative) and SARS-CoV-2 infected (positive) patients
743 was obtained from the laboratory of virology of the Purpan hospital, as previously described
744 (Abravanel et al. 2020).
745 Rangueil Cohort: The samples were routine care residues from random patients, anonymized
746 within 48 hours of collection, regardless of gender or hospitalization reason, collected in the
747 course of a month between the end of January and the end of February 2021. The Covid status
748 (PCR or positive serology) was unknown to the person performing the Jurkat-S&R-flow, ELISA
749 and HAT experiments. Those whole blood samples were kept at room temperature until being
750 used for HAT assays within 24 hours of obtaining them from the hospital. In trial experiments,
751 we had found that such samples could be stored for up to 5 days without any noticeable
752 difference in the performance of the HAT test.
753 After the whole blood samples had been used for HAT assays, the tubes were then spun, and
754 the plasmas harvested into fresh tubes (to which sodium azide was added at a final
755 concentration of 200 ug/ml). Those harvested plasmas were kept at 4°C until they were used to
756 perform the Jurkat-S&R-flow tests and ELISA tests.

757 Capillary blood: one of the authors of this study collected 50 µL of his own blood by finger
758 pricking, using disposable lancets (Sarstedt ref 85.1016) on various days during the course of
759 his vaccination regimen with the Pfizer/BioNTech vaccine. At the time of collection, the blood
760 samples were diluted with 200 µL of PBS + 5mM EDTA (Since whole blood is roughly 50% RBCs
761 and 50% plasma, this 1/5 dilution of the blood actually corresponds to a 1/10 dilution of the
762 plasma). The plasma was then separated from the RBCs after centrifugation, placed in another
763 tube with sodium azide, and stored at 4°C until the day of the assay.
764
765 **Experiments on mouse sera**
766 Virus preparation and inactivation
767 SARS-CoV2 was grown on Vero E6 cells (ATCC) in DMEM (Dutscher) supplemented with
768 100 U/mL penicillin, 100 µg/ml streptomycin (Invitrogen), and 2% heat inactivated fetal bovine
769 serum (Sigma). Viral stocks were propagated in 300 cm^2 flasks (Dutscher) in which 10^3 tissue
770 culture infectious dose 50 ($TCID_{50}$) were inoculated in 100 ml of medium for 3 days at 37°C with
771 5% CO_2. Culture supernatants containing the viral stocks were harvested and inactivated with
772 BPL (Fischer) overnight at 4°C. Virus was then concentrated by ultracentrifugation at 25 000 rpm
773 (for 2 hours at 4°C) on a 20% sucrose cushion in Ultra-Clear centrifuge tubes (SW-32 Ti rotor,
774 Beckman). Pellets were resuspended in PBS, protein concentration was quantified by BCA
775 Protein Assay kit (Pierce). BPL-inactivated SARS-CoV2 stocks at protein concentrations ranging
776 from 1 to 5 µg/µL were stored at -80°C until use.
777 Mouse immunization
778 Mice were injected intra-peritoneally with 15 µg of BPL-SARS-CoV2 in 250 µl of PBS, and then
779 challenged with the same amount at day 62. Mice were euthanized and serum was collected at
780 day 14 post-primary immunization and at day 7 post-secondary challenge.
781
782 **Experiments on Cat and Dog sera**
783 Serum samples were collected from cats and dogs belonging to owners who developed COVID-
784 19-like symptoms and subsequently tested positive for SARS-CoV-2 infection by RT-qPCR. , at least
785 one month after the owners' recoveries. Samples and data collections were conducted according
786 to the guidelines of the Declaration of Helsinki, and approved by the Ethics Committee Sciences
787 et Santé Animale n◦115 (protocol code COVIFEL approved on 1 September 2020, registered under
788 SSA_2020_010).
789 Sero-neutralisation assay
790 Serum samples and controls were heat-inactivated at 56 °C for 30 min, serially diluted in
791 DMEM starting at 1:10, mixed with an equal volume of SARS-CoV-2 stock (previously amplified
792 and titrated on Vero-E6 cells and diluted in DMEM to contain 2000 $TCID_{50}$/ml), incubated for 2
793 hours at 37 °C, and 100 µL transferred to tissue-culture 96 well plates plated with 12.000 Vero-
794 E6 cells per well the day before the assay, in DMEM complemented with 10% of heat-
795 inactivated fetal bovine serum and 1% of penicillin-streptomycin at 37 °C with 5% of CO2
796 (medium was removed before adding the virus-serum dilutions). After 60 minutes at 37°C, the
797 virus-serum dilutions were removed before adding DMEM complemented with 2% of heat-
798 inactivated fetal bovine serum and 1% of penicillin-streptomycin. Cells were then incubated for
799 72 h at 37 °C with 5% of CO2. Individual wells were then screened by eye under the microscope
800 for cytopathic effects. Monoclonal anti-SARS-CoV CR3022 antibody (BEI Resources, NIAID, NIH)
801 was used as a positive control. PBS was used as a negative control. Experiments were carried
802 out in a biosafety level 3 facility at the National Veterinary School of Toulouse.

Ethical statement

All sera from the first cohort, and whole blood samples from the second cohort, were obtained from the Toulouse hospital, where all patients give, by default, their consent for any biological material left over to be used for research purposes after all the clinical tests requested by doctors have been duly completed. Material transfer was done under a signed agreement (CNRS n° 227232, CHU n° 20 427 C). This study was declared and approved by the governing body of the Toulouse University Hospital with the agreement number RnIPH 2021-99, confirming that ethical requirements were fully respected.

Using such materials, we did not really have control over how representative our cohorts may be, but this allowed us to circumvent the very stringent rules set by French laws regarding the use of human materials for research (RIPH, Loi Jardé). Under those rules, setting up a clinical trial involving biological materials of human origin would require many months of administrative procedures and paperwork, as well as several hundreds of thousands of euros, which we did not have access to.

Bibliography

Abravanel, F., Miédouge, M., Chapuy-Regaud, S., Mansuy, J.-M. and Izopet, J. 2020. Clinical performance of a rapid test compared to a microplate test to detect total anti SARS-CoV-2 antibodies directed to the spike protein. *Journal of Clinical Virology* 130, p. 104528.

Abu-Raddad, L.J., Chemaitelly, H., Coyle, P., et al. 2021. SARS-CoV-2 reinfection in a cohort of 43,000 antibody-positive individuals followed for up to 35 weeks. *medRxiv*.

Adams, E.R., Ainsworth, M., Anand, R., et al. 2020. Antibody testing for COVID-19: A report from the National COVID Scientific Advisory Panel. *Wellcome Open Research* 5, p. 139.

Amanat, F., Stadlbauer, D., Strohmeier, S., et al. 2020. A serological assay to detect SARS-CoV-2 seroconversion in humans. *Nature Medicine* 26(7), pp. 1033–1036.

Barnes, C.O., Jette, C.A., Abernathy, M.E., et al. 2020. SARS-CoV-2 neutralizing antibody structures inform therapeutic strategies. *Nature* 588(7839), pp. 682–687.

Bessière, P., Fusade-Boyer, M., Walch, M., et al. 2021. Household Cases Suggest That Cats Belonging to Owners with COVID-19 Have a Limited Role in Virus Transmission. *Viruses* 13(4).

Chen, H. 2020. Susceptibility of ferrets, cats, dogs, and different domestic animals to SARS-coronavirus-2. *BioRxiv*.

Chen, Xinhua, Chen, Z., Azman, A.S., et al. 2021. Serological evidence of human infection with SARS-CoV-2: a systematic review and meta-analysis. *The Lancet. Global health* 9(5), pp. e598–e609.

Dejnirattisai, W., Zhou, D., Ginn, H.M., et al. 2021. The antigenic anatomy of SARS-CoV-2 receptor binding domain. *Cell* 184(8), p. 2183–2200.e22.

Dortet, L., Ronat, J.-B., Vauloup-Fellous, C., et al. 2021. Evaluating 10 Commercially Available SARS-CoV-2 Rapid Serological Tests by Use of the STARD (Standards for Reporting of Diagnostic Accuracy Studies) Method. *Journal of Clinical Microbiology* 59(2).

Dróżdż, M., Krzyżek, P., Dudek, B., Makuch, S., Janczura, A. and Paluch, E. 2021. Current State of Knowledge about Role of Pets in Zoonotic Transmission of SARS-CoV-2. *Viruses* 13(6).

Egia-Mendikute, L., Bosch, A., Prieto-Fernández, E., et al. 2021. Sensitive detection of SARS-CoV-2 seroconversion by flow cytometry reveals the presence of nucleoprotein-reactive antibodies in unexposed individuals. *Communications Biology* 4(1), p. 486.

Fani, M., Teimoori, A. and Ghafari, S. 2020. Comparison of the COVID-2019 (SARS-CoV-2) pathogenesis with SARS-CoV and MERS-CoV infections. *Future virology*.

851 Farnsworth, C.W. and Anderson, N.W. 2020. SARS-CoV-2 Serology: Much Hype, Little Data.
852 *Clinical Chemistry* 66(7), pp. 875–877.
853 Feng, S., Phillips, D.J., White, T., et al. 2021. Correlates of protection against symptomatic and
854 asymptomatic SARS-CoV-2 infection. *medRxiv*.
855 Garcia-Beltran, W.F., Lam, E.C., Astudillo, M.G., et al. 2021. COVID-19-neutralizing antibodies
856 predict disease severity and survival. *Cell* 184(2), p. 476–488.e11.
857 Goh, Y.S., Ng, L.F.P. and Renia, L. 2021. A flow cytometry-based assay for serological
858 detection of anti-spike antibodies in COVID-19 patients. *STAR Protocols* 2(3), p. 100671.
859 Grzelak, L., Temmam, S., Planchais, C., et al. 2020. A comparison of four serological assays for
860 detecting anti-SARS-CoV-2 antibodies in human serum samples from different populations.
861 *Science Translational Medicine* 12(559).
862 Hambach, J., Stähler, T., Eden, T., et al. 2021. A simple, sensitive, and low-cost FACS assay for
863 detecting antibodies against the native SARS-CoV-2 spike protein. *Immunity, inflammation*
864 *and disease* 9(3), pp. 905–917.
865 Harvey, R.A., Rassen, J.A., Kabelac, C.A., et al. 2021. Association of SARS-CoV-2 Seropositive
866 Antibody Test With Risk of Future Infection. *JAMA internal medicine* 181(5), pp. 672–679.
867 Harvey, W.T., Carabelli, A.M., Jackson, B., et al. 2021. SARS-CoV-2 variants, spike mutations
868 and immune escape. *Nature Reviews. Microbiology* 19(7), pp. 409–424.
869 Hickey, M.J., Valenzuela, N.M. and Reed, E.F. 2016. Alloantibody generation and effector
870 function following sensitization to human leukocyte antigen. *Frontiers in immunology* 7, p.
871 30.
872 Horndler, L., Delgado, P., Abia, D., et al. 2021. Flow cytometry multiplexed method for the
873 detection of neutralizing human antibodies to the native SARS-CoV-2 spike protein. *EMBO*
874 *Molecular Medicine* 13(3), p. e13549.
875 Huang, K.-Y.A., Tan, T.K., Chen, T.-H., et al. 2021. Breadth and function of antibody response
876 to acute SARS-CoV-2 infection in humans. *PLoS Pathogens* 17(2), p. e1009352.
877 Jayathilaka, D., Jeewandara, C., Gomes, L., et al. 2021. Comparison of kinetics of immune
878 responses to SARS-CoV-2 proteins in individuals with varying severity of infection and
879 following a single dose of the AZD1222. *medRxiv*.
880 Jeewandara, C., Kamaladasa, A., Pushpakumara, P.D., et al. 2021. Immune responses to a single
881 dose of the AZD1222/Covishield vaccine in health care workers. *Nature Communications*
882 12(1), p. 4617.
883 Jeffery-Smith, A., Iyanger, N., Williams, S.V., et al. 2021. Antibodies to SARS-CoV-2 protect
884 against re-infection during outbreaks in care homes, September and October 2020. *Euro*
885 *Surveillance* 26(5).
886 Kamaladasa, A., Gunasekara, B., Jeewandara, C., et al. 2021. Comparison of two assays to detect
887 IgG antibodies to the receptor binding domain of SARS-CoV-2 as a surrogate marker for
888 assessing neutralizing antibodies in COVID-19 patients. *International Journal of Infectious*
889 *Diseases* 109, pp. 85–89.
890 Karahan, G.E., Claas, F.H.J. and Heidt, S. 2020. Pre-existing Alloreactive T and B Cells and
891 Their Possible Relevance for Pre-transplant Risk Estimation in Kidney Transplant Recipients.
892 *Frontiers in medicine* 7, p. 340.
893 Khan, S., Nakajima, R., Jain, A., et al. 2020. Analysis of Serologic Cross-Reactivity Between
894 Common Human Coronaviruses and SARS-CoV-2 Using Coronavirus Antigen Microarray.
895 *BioRxiv*.
896 Khoury, D.S., Cromer, D., Reynaldi, A., et al. 2021. Neutralizing antibody levels are highly
897 predictive of immune protection from symptomatic SARS-CoV-2 infection. *Nature Medicine*
898 27(7), pp. 1205–1211.
899 Koopmans, M. and Haagmans, B. 2020. Assessing the extent of SARS-CoV-2 circulation

900 through serological studies. *Nature Medicine* 26(8), pp. 1171–1172.
901 Lamikanra, A., Nguyen, D., Simmonds, P., et al. 2021. Comparability of six different
902 immunoassays measuring SARS-CoV-2 antibodies with neutralising antibody levels in
903 convalescent plasma: from utility to prediction. *Transfusion*.
904 Lapuente, D., Maier, C., Irrgang, P., et al. 2021. Rapid response flow cytometric assay for the
905 detection of antibody responses to SARS-CoV-2. *European Journal of Clinical Microbiology*
906 *& Infectious Diseases* 40(4), pp. 751–759.
907 Letizia, A.G., Ge, Y., Vangeti, S., et al. 2021. SARS-CoV-2 Seropositivity and Subsequent
908 Infection Risk in Healthy Young Adults: A Prospective Cohort Study. *SSRN Electronic*
909 *Journal*.
910 Long, Q.-X., Tang, X.-J., Shi, Q.-L., et al. 2020. Clinical and immunological assessment of
911 asymptomatic SARS-CoV-2 infections. *Nature Medicine* 26(8), pp. 1200–1204.
912 Lumley, S.F., O'Donnell, D., Stoesser, N.E., et al. 2021. Antibody Status and Incidence of
913 SARS-CoV-2 Infection in Health Care Workers. *The New England Journal of Medicine*
914 384(6), pp. 533–540.
915 ter Meulen, J., van den Brink, E.N., Poon, L.L.M., et al. 2006. Human monoclonal antibody
916 combination against SARS coronavirus: synergy and coverage of escape mutants. *PLoS*
917 *Medicine* 3(7), p. e237.
918 Mohit, E., Rostami, Z. and Vahidi, H. 2021. A comparative review of immunoassays for COVID-
919 19 detection. *Expert review of clinical immunology*.
920 Moshe, M., Daunt, A., Flower, B., et al. 2021. SARS-CoV-2 lateral flow assays for possible use
921 in national covid-19 seroprevalence surveys (React 2): diagnostic accuracy study. *BMJ*
922 *(Clinical Research Ed.)* 372, p. n423.
923 Ng, K.W., Faulkner, N., Cornish, G.H., et al. 2020. Preexisting and de novo humoral immunity to
924 SARS-CoV-2 in humans. *Science* 370(6522), pp. 1339–1343.
925 Piccoli, L., Park, Y.-J., Tortorici, M.A., et al. 2020. Mapping Neutralizing and Immunodominant
926 Sites on the SARS-CoV-2 Spike Receptor-Binding Domain by Structure-Guided High-
927 Resolution Serology. *Cell* 183(4), p. 1024–1042.e21.
928 Piñero, P., Marco De La Calle, F.M., Horndler, L., et al. 2021. Flow cytometry detection of
929 sustained humoral immune response (IgG + IgA) against native spike glycoprotein in
930 asymptomatic/mild SARS-CoV-2 infection. *Scientific Reports* 11(1), p. 10716.
931 Robbiani, D.F., Gaebler, C., Muecksch, F., et al. 2020. Convergent antibody responses to SARS-
932 CoV-2 in convalescent individuals. *Nature* 584(7821), pp. 437–442.
933 Sit, T.H.C., Brackman, C.J., Ip, S.M., et al. 2020. Infection of dogs with SARS-CoV-2. *Nature*
934 586(7831), pp. 776–778.
935 Townsend, A., Rijal, P., Xiao, J., et al. 2021. A haemagglutination test for rapid detection of
936 antibodies to SARS-CoV-2. *Nature Communications* 12(1), p. 1951.
937 Wu, Z., Harrich, D., Li, Z., Hu, D. and Li, D. 2021. The unique features of SARS-CoV-2
938 transmission: Comparison with SARS-CoV, MERS-CoV and 2009 H1N1 pandemic influenza
939 virus. *Reviews in medical virology* 31(2), p. e2171.
940 Zhou, D., Duyvesteyn, H.M.E., Chen, C.-P., et al. 2020. Structural basis for the neutralization of
941 SARS-CoV-2 by an antibody from a convalescent patient. *Nature Structural & Molecular*
942 *Biology* 27(10), pp. 950–958.

Supplementary material

Figure S1

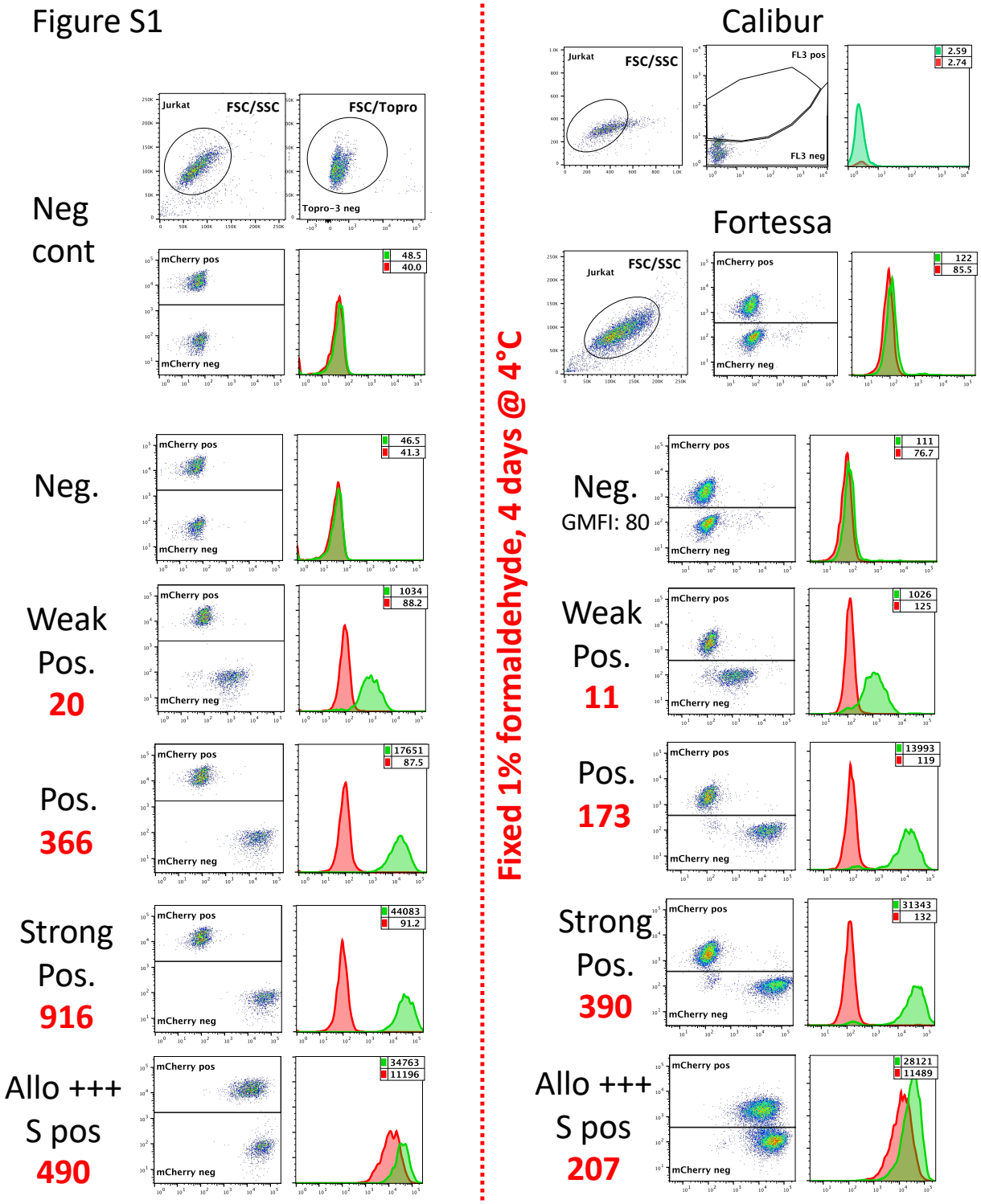

947 **Figure S1**: Using a flow cytometer with a 561 nm Yellow-Green laser improves the mCherry
948 signals
949 The same samples shown on Figure 1 were also analyzed on a Fortessa flow cytometer. The
950 561 nm yellow-green laser was used for the excitation of the mCherry fluorescent protein,
951 which led to much brighter signals, and thus to much easier separation of the Jurkat-R (mCherry
952 pos) and Jurkat-S (mCherry neg) populations than when the samples were acquired on a
953 FACScalibur.
954 As in figure 1, the numbers in the upper right corners of the histogram overlays plots
955 correspond to the GMFI of the two histograms (Red: Jurkat-R; green: Jurkat-S), and the big red
956 numbers to the left of the plots to the RSS. Of note, although the GMFI values were much higher
957 on the Fortessa than those recorded on the FACScalibur, the RSS values of the various samples
958 were all very similar between the two machines.
959
960 After the samples had been run on both flow cytometers, those were fixed in 1%
961 formaldehyde by adding an equal volume of PBS + 2% formaldehyde to the remainder of each
962 sample. The tubes were then stored à 4°C for 4 days before re-analyzing them on both
963 cytometers. As can be seen on the right hand side of the figure, the red fluorescence of the
964 mCherry was still detectable on the Fortessa after this procedure of fixation, despite the
965 intensity of the signals having dropped by about 7 fold. On the FACScalibur, however, this drop
966 of the mCherry fluorescent signals precluded the separation of the Jurkat-S from the Jurkat-R
967 cells. If samples are to be fixed, performing the Jurkat-R&S-flow test will thus require access to a
968 flow cytometer equipped with a 561 nm Yellow-Green laser. As an alternative, we are currently
969 exploring the possibility of transforming the Jurkat-S&R-flow test into a Jurkat-S&G-flow test,
970 where the negative control cells would be expressing GFP, which is excited at 488 nm, and using
971 secondary antibodies conjugated to red fluorochromes such as Alexa647, excited by a 633 nm
972 red laser, for the detection of the primary antibodies.
973
974 Of note, in the dot plots of the Positive and Strong Positive fixed samples, faint clouds of FL1
975 negative cells can be seen in the mCherry neg window. Those presumably correspond to Jurkat-
976 R cells which were dead before the fixation step, and from which the mCherry had thus leaked
977 out. When analyzing populations of live cells, such cells are gated out with the To-pro 3 live
978 stain, but this no longer works for population of fixed cells. This small problem could probably
979 be circumvented using a fixable dead cell staining dye such as the LIVE/DEAD Fixable Far Red
980 stain (ThermoFischer L34973).
981
982

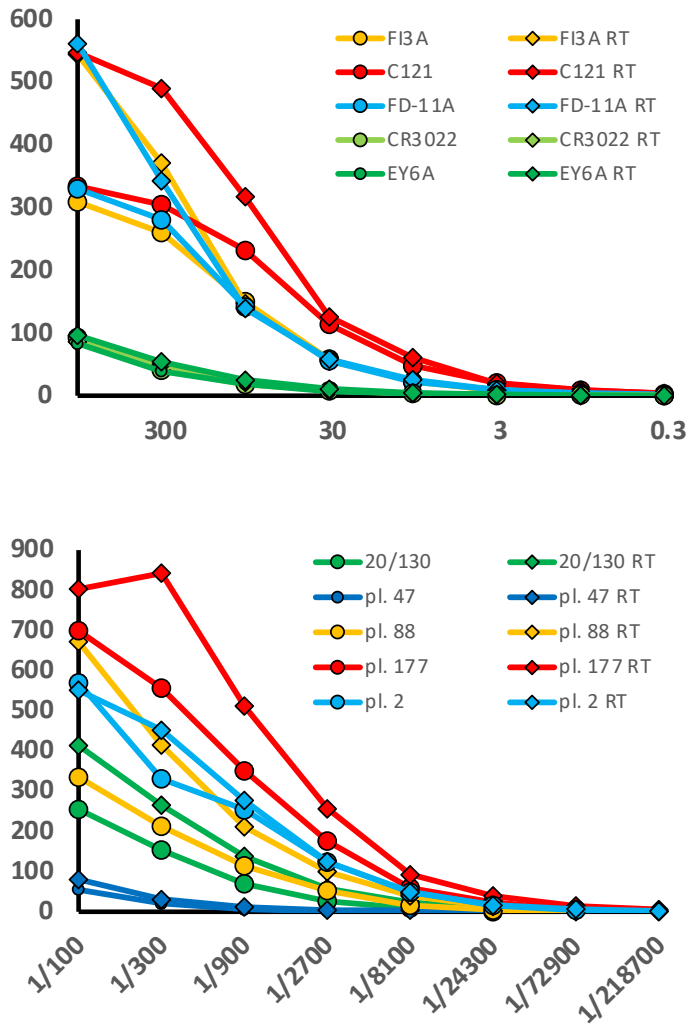

Figure S2: Incubation of the samples at room temperature for the first part of the primary staining step markedly improves the staining signals for most antibodies.

For a large fraction of monoclonal and polyclonal antibodies reacting with the Spike protein expressed at the surface of cells, we have repeatedly observed that a step of incubation at room temperature can result in a marked improvement of the staining signals compared to performing the staining continuously on ice.

For this experiment, we selected a panel of 5 monoclonal antibodies reacting with different sites of the spike RBD domain, a panel of 4 plasmas reacting with various intensities, as well the 20/130 reference serum.

For all the samples, we performed eight steps of 3-fold dilutions, and placed 10 ul of the diluted samples in two parallel U bottom 96 well plates. The first plate was kept at room temperature (RT) whilst the other one was placed on ice. The Jurkat-S&R mix was then added to the wells of the plate at room temperature. The tube was then placed on ice for a few minutes, before distributing the mix in the wells of the second plate. After 30 minutes, the plate which had been sitting at room temperature was also placed on ice, and incubated for another 30 minutes. The rest of the staining procedure was then exactly the same for the two plates, all performed in the cold as described in M&M.

		IgGAM			IgG			IgA			IgM						
	Sample ID	GMFI Jurkat-R	GMFI Jurkat-S	specific stain (J-S - J-R)	GMFI Jurkat-R	GMFI Jurkat-S	specific stain (J-S - J-R)	GMFI Jurkat-R	GMFI Jurkat-S	specific stain (J-S - J-R)	GMFI Jurkat-R	GMFI Jurkat-S	specific stain (J-S - J-R)	G+A+M	Fraction IgG signal	Fraction IgA signal	Fraction IgM signal
	neg	1.87	2.01	0.14	1.95	1.99	0.04	1.79	2.13	0.34	1.89	1.98	0.09	0.47			
Sera	**30/120**	3.19	760	756.81	3.59	763	759.41	2.11	63.2	61.09	2.74	640	637.26	1457.76	0.52	0.04	0.44
	<J14-3	5.1	51.6	46.5	7.47	57.2	49.73	3.08	29.1	26.02	2.55	8.65	6.1	81.85	0.61	0.32	0.07
	<J14-29	4.59	738	733.41	5.16	919	913.84	2.77	122	119.23	2.54	203	200.46	1233.53	0.74	0.10	0.16
	<J14-32	4.71	1692	1687.29	5.25	2350	2344.75	4.01	610	605.99	2.56	402	399.44	3350.18	0.70	0.18	0.12
	<J14-35	4.65	198	193.35	4.82	209	204.18	1.97	52.6	50.63	3.14	13.1	9.96	264.77	0.77	0.19	0.04
	<J14-109	6.52	852	845.48	6.23	1082	1075.77	2.61	179	176.39	4.55	126	121.45	1373.61	0.78	0.13	0.09
	<J14-130	8.7	150	141.3	9.46	151	141.54	3.28	45.7	42.42	5.25	58.1	52.85	236.81	0.60	0.18	0.22
	>J14-40	4.84	54.9	50.06	6.07	54.3	48.23	2.18	12	9.82	2.76	29.1	26.34	84.39	0.57	0.12	0.31
	neg-2213	10.5	33.3	22.8	12.3	43.3	31	3.21	6.58	3.37	6.12	8.77	2.65	37.02	0.84	0.09	0.07
	neg-2649	19.2	41.4	22.2	24.7	56.2	31.5	6.32	9.59	3.27	6.15	9.62	3.47	38.24	0.82	0.09	0.09
Plasmas	**2**	438	1427	989	577	1846	1269	59.4	469	409.6	739	1333	594	2272.60	0.56	0.18	0.26
	18	7.82	84.9	77.08	11.3	101	89.7	2.67	33.4	30.73	4.89	12.7	7.81	128.24	0.70	0.24	0.06
	19	2.02	2.2	0.18	2.07	2.15	0.08	1.82	2.18	0.36	1.83	1.96	0.13	0.57			
	36	4.53	88.7	84.17	5.01	90.2	85.19	2.38	48.5	46.12	3.61	10.4	6.79	138.10	0.62	0.33	0.05
	47	3.47	139	135.53	3.65	141	137.35	2.15	47.1	44.95	2.8	42.2	39.4	221.70	0.62	0.20	0.18
	56	9.03	25.7	16.67	9.48	26.8	17.32	2.56	17.2	14.64	7.16	11.2	4.04	36.00	0.48	0.41	0.11
	57	5.84	25.5	19.66	7.04	26.7	19.66	2.17	8.87	6.7	4.55	13.9	9.35	35.71	0.55	0.19	0.26
	73	3.87	130	126.13	3.61	159	155.39	1.91	4.35	2.44	3.1	4.64	1.54	159.37	0.98	0.02	0.01
	80	2.5	82	79.5	3.07	99.1	96.03	2.06	2.75	0.69	2.21	2.56	0.35	97.07	0.99	0.01	0.00
	83	3.13	1674	1670.87	3.69	1900	1896.31	2.21	542	539.79	2.4	629	626.6	3062.70	0.62	0.18	0.20
	88	3.74	1110	1106.26	4.18	1297	1292.82	2.51	159	156.49	3.03	632	628.97	2078.28	0.62	0.08	0.30
	108	3.53	7.65	4.12	4.22	9.66	5.44	2.08	2.61	0.53	2.6	3.58	0.98	6.95			
	123	54.5	75.6	21.1	51.6	71.4	19.8	4.22	6.14	1.92	43.5	61.1	17.6	39.32	0.62	0.08	0.30
	161	2.91	5.84	2.93	6.17	11.1	4.93	2.08	2.59	0.51	2.09	2.25	0.16	5.60			
	166	101	162	61	109	176	67	27.2	35.3	8.1	46.5	68.9	22.4	97.50	0.69	0.08	0.23
	174	3.11	190	186.89	4.43	228	223.57	2.45	50.1	47.65	2.19	42.3	40.11	311.33	0.72	0.15	0.13
	177	7.9	1945	1937.1	8.04	2303	2294.96	2.32	581	578.68	7.58	699	691.42	3565.06	0.64	0.16	0.19
	227	4.12	77	72.88	5.31	51.4	46.09	2.83	6.19	3.36	3	73.8	70.8	120.25	0.38	0.03	0.59
	232	11	131	120	12.6	169	156.4	6.21	9.13	2.92	4.84	6.83	1.99	161.31	0.97	0.02	0.01
	241	4.11	2411	2406.89	4.61	2860	2855.39	2.6	608	605.4	2.83	47.8	44.97	3505.76	0.81	0.17	0.01
	247	13.8	23.3	9.5	21.6	31.7	10.1	8.87	15.7	6.83	3.5	5.88	2.38	19.31	0.52	0.35	0.12
	253	3.98	28.2	24.22	5.22	33	27.78	2.43	10.7	8.27	2.43	2.9	0.47	36.52	0.76	0.23	0.01
	260	23.2	33.9	10.7	30.8	44.1	13.3	29.4	43	13.6	5.98	7.61	1.63	28.53	0.47	0.48	0.06

Table S1: Example of isotyping performed on a representative set of various serum and plasma samples.

As can be seen on the right hand side portion of the table, comparison of samples from different patients shows that there can be large variations in the proportions of Ig-G,-A and -M. Because polyclonal secondary antibodies will not all react with their targeted primary antibodies with the same efficiency, however, the actuals signals for the various subclasses of antibodies should not be taken as a true reflection of the amounts of each subclass of antibody.

If a more quantitative evaluation was needed, monoclonal secondary antibodies could be used instead of polyclonal reagents, making sure that all those isotypes-specific secondary monoclonal antibodies were being used well above the saturating concentration, and conjugated to similar amounts of the same fluorochrome. This would, however, increase the cost of the procedure considerably.